Environ Earth Sci (2013) 70:281–293
DOI 10.1007/s12665-012-2126-9

ORIGINAL ARTICLE

Groundwater flow and radioactivity in Namaqualand, South Africa

Tamiru A. Abiye · Joyce T. Leshomo

Received: 21 June 2012 / Accepted: 14 November 2012 / Published online: 29 November 2012

Abstract The Namaqualand area is located in the Northern Cape Province of South Africa which is characterised by arid climate where groundwater is the only source of water supply for local communities. Extensive groundwater sampling was carried out in the area and the physico-chemical parameters, inorganic constituents, stable isotopes and trace metals were measured. The hydrochemistry of the area indicates dissimilar groundwater composition due to complex geochemical processes where groundwater flow takes place from catchment F30A to the catchment D82B, and the chemistry is controlled primarily by Redox reaction, dissolution and mixing processes. The Br^-/Cl^- ratio revealed that the salinity in the area is derived from seawater mixing, halite dissolution and atmospheric deposition/sea aerosol spray. Under excessive evaporative condition due to climatic aridity, groundwater salinity shows increasing trend. Isotope results show the presence of shallow-weathered zone and deep-fracture controlled circulating groundwater in the crystalline basement aquifer of the area. In comparison to the South African water quality standard, the results obtained for gross alpha activity which could be derived from uranium isotopes show that 41 % of the reported data in the area fall above the drinking water limit.

Keywords Arid environment · Groundwater flow · Radioactivity · Uranium · South Africa

T. A. Abiye (✉)
School of Geosciences, University of the Witwatersrand, Private Bag X3, P.O. Box Wits 2050, Johannesburg, South Africa
e-mail: tamiru.abiye@wits.ac.za

J. T. Leshomo
Council for Geosciences, 280 Pretoria St, Pretoria 0001, South Africa

Introduction

The demand for groundwater in South Africa has increased over the years, particularly in the arid, semi-arid and rural areas of the country (Titus et al. 2009) that includes the Namaqualand area, which lies in the driest south-western part of the country (Fig. 1). The study area falls within the Bushmanland area identified as catchment F30A and D82B in the Northern Cape Province of South Africa.

Due to the lack of safe surface water supply in the area, people rely on groundwater which is impacted by mineralization processes. Chemical constituents that increase the salinity and change in the groundwater quality are introduced into the aquifer primarily through parent rock weathering and dissolution and anthropogenic sources. It is presumed that natural geological source could be the cause for the groundwater quality deterioration in the area, which is supplemented by climatic aridity.

According to Cole (1998), there are two principal types of uranium deposits in the Northern Cape Province: the one associated with granites and pegmatites of the Namaqualand Metamorphic Complex, and the second surficial deposit which occur in the tertiary to recent fluvial and alluvial sediments. Cole (1998) has also reported that the granite, leucogranites and gneiss of the Namaqualand Metamorphic complex contain high uranium concentrations. Pegmatitic and aplitic rocks show secondary enrichment towards surface, where uraniferous thorianite ($ThSiO_4$) is a major thorium and uranium-bearing mineral (Cole 1998). Uranium-bearing pegmatites are found mainly intruding granitic gneiss in the Namaqualand Metamorphic Complex with values of up to 2660 ppm (Cole 1998). Pegmatites also host a variety of minerals containing thorium together with other base metals of economic importance (e.g. beryl, colombinte-tantalite lithium and

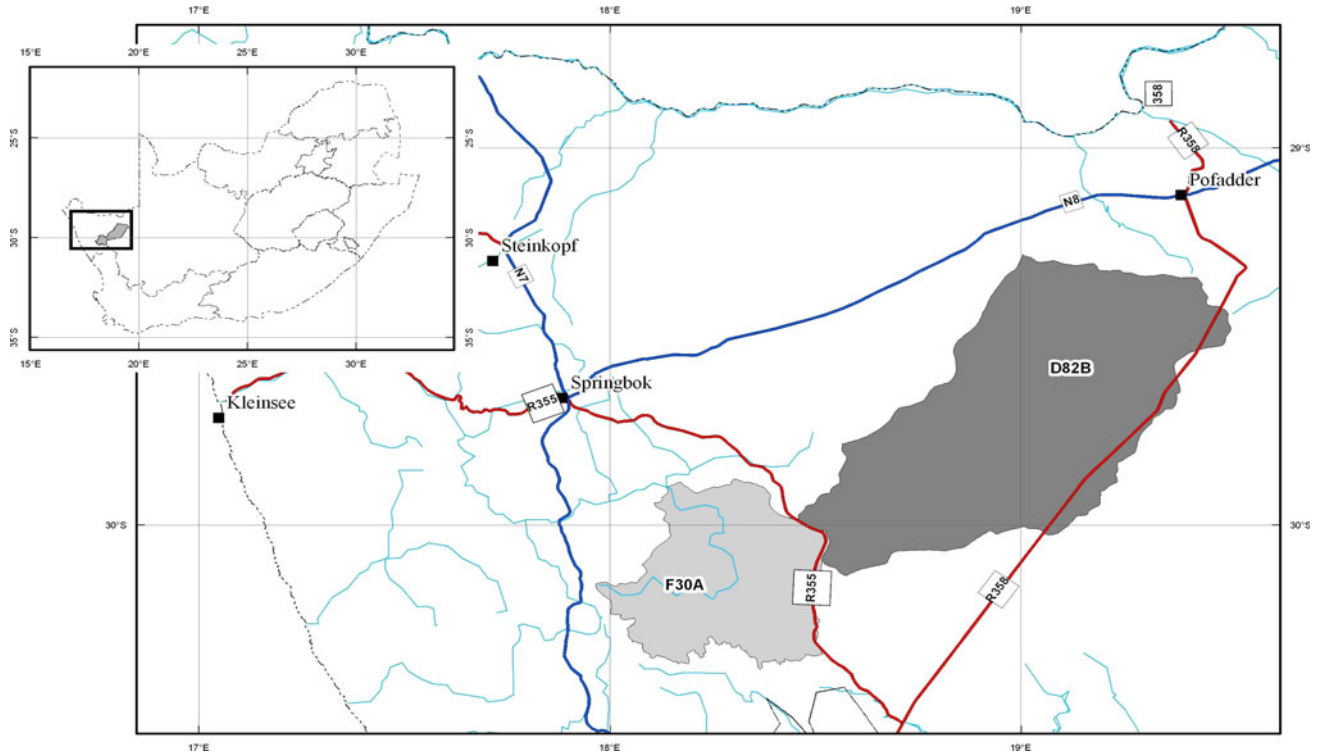

Fig. 1 Location map of catchment F30A and D28B, in Namaqualand, Northern Cape Province, South Africa

bismuth-bearing minerals, mica, feldspars, etc.) (Frick 1986).The Concordia granite hosts high uranium content (35–70 ppm) as compared to other granites in the area (Cole 1998). Alaskites have even higher uranium content which lies between 20 and 450 ppm (Cole 1998). The prime uranium-bearing minerals are quartz and alkali feldspars, and the other minerals where uranium was found are biotite, zircon, magnetite, monazite, gadolinite and niobium-tantalum oxide phases (Cole 1998). The lacustrine deposits provide uraninite and urano-organic complexes with carnotite being the main uranium mineral (Cole 1998). The carnotite mineral is said to be derived from the gneiss of the Namaqua Metamorphic Province (Agenbacht 2007). Other anomalies are associated with the Dwyka Group with uranium values of up to 210 ppm (Cole 1998). The uranium is apparently incorporated in apatite crystals within nodules of calcareous mudrock that has concentration of 950 ppm (Cole 1998). Andreoli et al. (2006) have reported a concentration of U and Th from charnokites rocks as 52 and 400 ppm, respectively. In the groundwater of Namaqualand, the presence of uranium was also reported by Toens et al. (1998).

In many parts of the world, Uranium was detected in groundwater pumped for community water supply. In Italy, around Gran Sasso massifs, the uranium concentration in groundwater varies between 0.1 and 50 μg/l which is derived from the weathering of U-bearing rocks such as organic shale and granites (Plastino et al. 2009). Water samples from Ulaanbaatar groundwater supply, Mongolia shows high concentration of Uranium (0.01–57 μg/l) where the concentration was associated with nephrotoxicity, high blood pressure, bone dysfunction and likely reproductive impairment in human populations (Nriagu et al. 2012). Groundwater samples collected at several spas in Saõ Paulo and Minas Gerais States in Brazil show that the gross alpha radioactivity ranges from 0.001 up to 0.4 Bq/l, while the gross beta radioactivity varies between 0.12 and 0.86 Bq/l (Bonotto et al. 2009). Uranium concentration of up to 0.17 μg/l was measured in the groundwater destined for human consumption in some part of Korea (Kim et al. 2004). Groundwater in the Kadugli area (West central Sudan) contain uranium radioactivity of 0.0161–1.720 Bq/l (Osman et al. 2008). The radioactivity related to uranium disintegration is also treated as toxic to human health. The gross alpha activity in the groundwater hosted by granitic aquifer around Eskisehir, Turkey ranges from 0.009 to 1.64 Bq/l (Örgün et al. 2005). Radioactivity in groundwater was also conducted as a precursor to providing a baseline of radiation exposure in arid-rural communities in Queensland, Australia, where U concentration of 0.71 Bq/l was registered (Kleinschmidt et al. 2011). High gross beta and alpha activities have also been reported for Guarani aquifer made of sedimentary rocks in Brazil (Bonotto and Bueno 2008).

The main purpose of this paper is to document the extent of trace metal distribution with particular emphasis to radioactivity in the groundwater which is used by local population for domestic and agricultural activities. Special emphasis has been given to hydrochemical evolution and processes that control groundwater mineralization.

Methodology

The methodologies applied in this assessment include analytical, radiological environmental isotopes and relating the obtained information with local site information. Boreholes were randomly selected for water sampling based on accessibility. Fifty-seven samples were collected from boreholes currently used for human and animal consumption. All water samples were filtered in the field with 0.45 μ filter. The samples were acidified immediately with HNO_3 to keep the metals mobile. The samples were kept cool in a dark place. Heavy metals in groundwater samples have been analysed by Perkin Elmer ELAN® DRC II ICP-MS system, equipped with a Meinhard nebulizer and a Cyclonic quartz spray chamber, was used in the analyses. Samples were introduced via Tygon® peristaltic pump tubing on a Perkin Elmer AS93 Plus auto-sampler, using a Type F auto-sampler tray capable of holding 148 sample vials of 16 ml each. An aliquot of sample was diluted in 50 ml polypropylene volumetric flasks with ultra-pure water (18.2 MΩ) and acidified with 2 % HNO_3 (AR grade). 20 ppb indium and 30 ppb iridium were added as internal standards. A suitable dilution factor was chosen for the sample's expected TDS and to match the calibration range of the instrument (normally 50 times dilution is sufficient). The water samples were diluted with Ultra-pure water (18.2 MΩ) and analysed for the anions F, Cl, NO_2, Br, NO_3, PO_4 and SO_4. Major ions were analysed by Dionex QIC Ion Chromatograph, equipped with an automated sampler and an IonPac AG4A guard column and IonPac AS4A analytical column.

A total of 57 rock/soil samples were collected close to the sampled borehole. In the absence of rock outcrop, soil samples were collected from trenches that lie at 15–20 cm in the boreholes. Heavy metal analysis has been performed using ICP-MS method at NECSA.

A 0.20 g portion of milled soil and rock sample was weighed into a Savillex container, and digested with 3 ml HCl, 2 ml HNO_3, 1 ml $HClO_4$ and 2 ml HF (all AR grade). The samples were heated on aluminium heating blocks at 110 °C to almost dry, and then at 160 °C until all acid evaporated (overnight). In addition, 1 ml of $HClO_4$ was added after 24 h and again evaporated at 160 °C. The residue was then dissolved with 1 ml HNO_3 and two drops H_2O_2. 19 ml of 1 % HNO_3 was then added, the sample containers was capped and then heated in an oven at 100 °C for 30 min. The dissolved samples were diluted again 20 times in polypropylene tubes with Indium and Iridium, added as internal standards, and analysed by ICP-MS.

Geological and hydrogeological overview

The Namaqualand area can be subdivided into three major geological provinces (Tankard et al. 1982). These are the basement rocks of the Namaqua Province, the volcano-sedimentary rocks of the Gariep Complex (Visser DJ 1989) in the northwest, and a Phanerozoic cratonic cover. The Namaqua Province represents most of the crystalline basement in the Northern Cape and Southern Namibia (Tankard et al. 1982). In Namaqualand, the margins of the Namaqua Province are largely obscured by younger cover rocks of the Gariep, Nama and Karoo sequences, as well as with Cenozoic surficial sediments to the east and west. In the west and in the north, rocks of the Namaqua Province and its correlatives are bordered by formations of the late Proterozoic Gariep Complex, and in the East with the Kaapvaal craton with marked structural discordance (Raith et al. 2003). In the south, rocks of the Nama Group, the Cape Supergroup and the lowermost units of the Karoo Supergroup cover the rocks of the Namaqua Province (Albat 1984). Rocks of the Central zone cover most of central Namaqualand and Bushmanland (including parts of northern and eastern Bushmanland) as well as the southwestern parts of southern Namibia (Tankard et al. 1982). The Bushmanland Group consists of granitic gneisses and a metamorphosed sequence of clastic shallow-water sediments, mafic to felsic volcanic rock and exhalites (Raith et al. 2003). The central zone of the Namaqua Province, a complex deformed heterogeneous group of gneisses and intrusions of medium to high grade metamorphism (Tankard et al. 1982) covers most of the Namaqua Province and comprises an assemblage of metasedimentary, metavolcanic and intrusive rocks (Fig. 2). Both catchments are mainly characterised by the sedimentary, volcanic and intrusive rocks of the Kheisian and Namaquan age which is mainly granites and gneisses. These rocks are overlain by the intrusive rocks of the Jurassic age, which are covered by sediments of the Tertiary and Quarternary age. The younger sediments are characterised by alluvium, pan sediments, calcareous and gypsiferous soil and aeolian sands.

The climatic aridity of the area is manifested by very low annual rainfall (≤200 mm/year) and has direct impact on the effective recharge. Hence, regional circulation is the sole source for aquifer replenishment. According to DWAF (2002) for catchment F30A and D82B, effective recharge is 5.8 and 19.5 mm/year, respectively. Even though, the recharge amount is very low, the report by DWAF (2002)

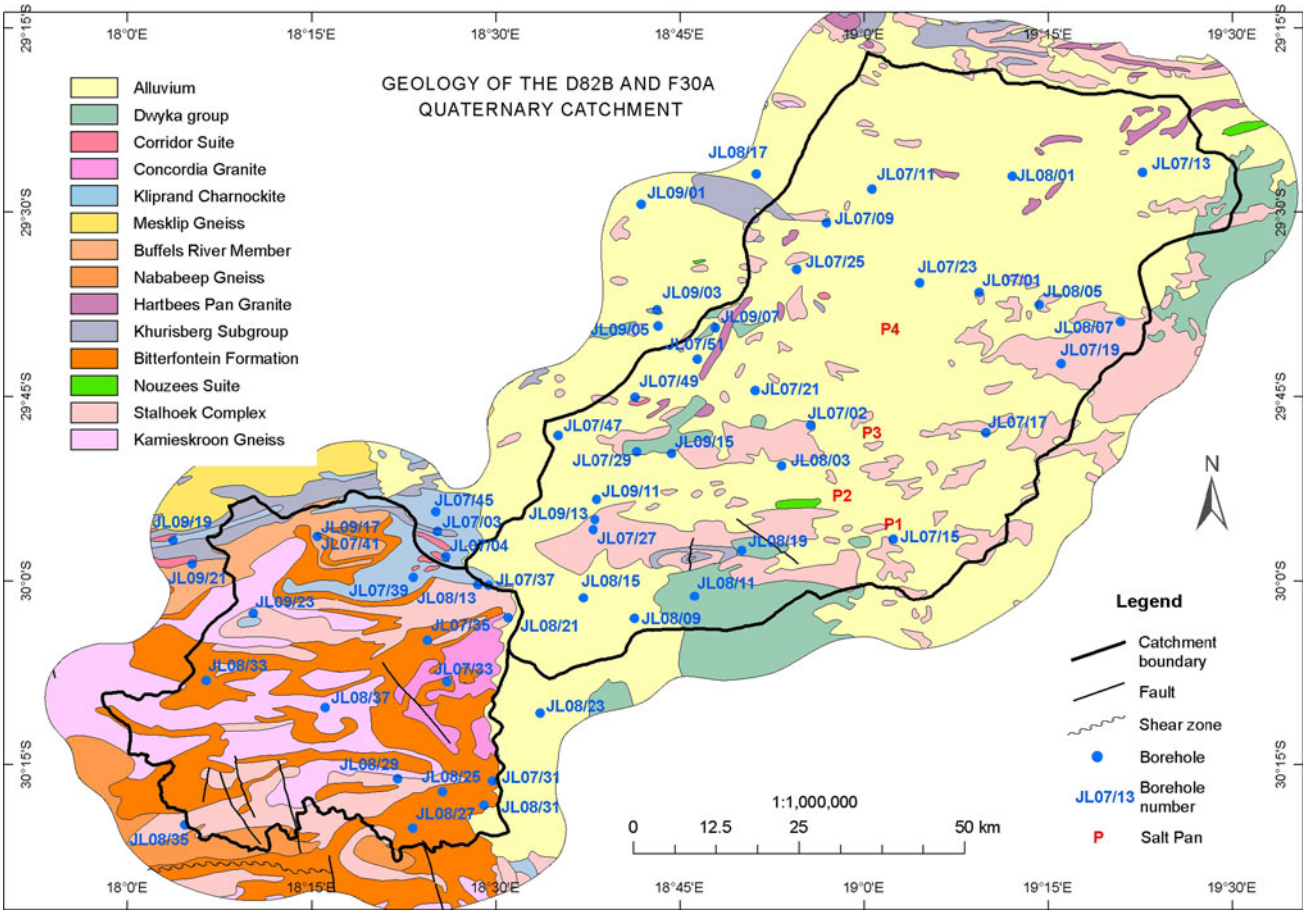

Fig. 2 Simplified geological map and borehole position in the area

shows that the total volume of aquifer storage in the F30A and D82B catchment is 91.4 M and 315.8 M m^3, respectively. Most of the boreholes in the area tap water from fractured basement aquifers. The aquifer extent and distribution in the area is largely controlled by the tectonics, fracture frequency, distribution of alluvial sediments and weathering zones.

The conceptual hydrogeological model (Fig. 3) which was constructed based on mean static water level data [22.22 m for F30A catchment and 36.45 m for D82B catchment (DWAF 2002)] shows that high topographic setting of catchment F30A derives recharge into the catchment D82B. It has been supported by the hydrochemical and isotope results (due to hydrochemical evolution direction from F30A into D82B catchment, mineral enrichment, and the presence of isotopically depleted water in D82B catchment).

Results and discussion

The analytical results for the physico-chemical and chemical constituents of the groundwater samples have been presented in Tables 1 and 2, while the uranium concentration for soil samples is portrayed in Fig. 4. The results revealed that the uranium concentration in 56 % of the groundwater samples fall above the WHO (World Health Organization) (2006) proposed drinking water standard which is 15 µg/l.

The obtained data further show that uranium concentration in the groundwater ranges between 3 and 146 µg/l, while in the soil/rock samples it ranges between 402 and 22,625 µg/l. Therefore, it is presumed that leaching process from soils and long term water–rock/soil interaction enriches the water supply aquifers with uranium and other trace metals.

The solubility of Uranium in aqueous systems is primarily controlled by: Redox, pH, and dissolved carbonate (Langmuir 1980; Murphy and Shock 1999) which controls its presence in the groundwater. The uranium stability field plot (Fig. 5) for the groundwater samples shows that uranium occurs in the form of UO_2^+ with few samples in UO_2OH^+, $U(OH)_5^-$ fields. The plot further reveals that the water samples plot on the deep groundwater zone (anaerobic media) with minimal direct recharge which implies the occurrence of regional recharge and complexation process for the uranium enrichment in the groundwater.

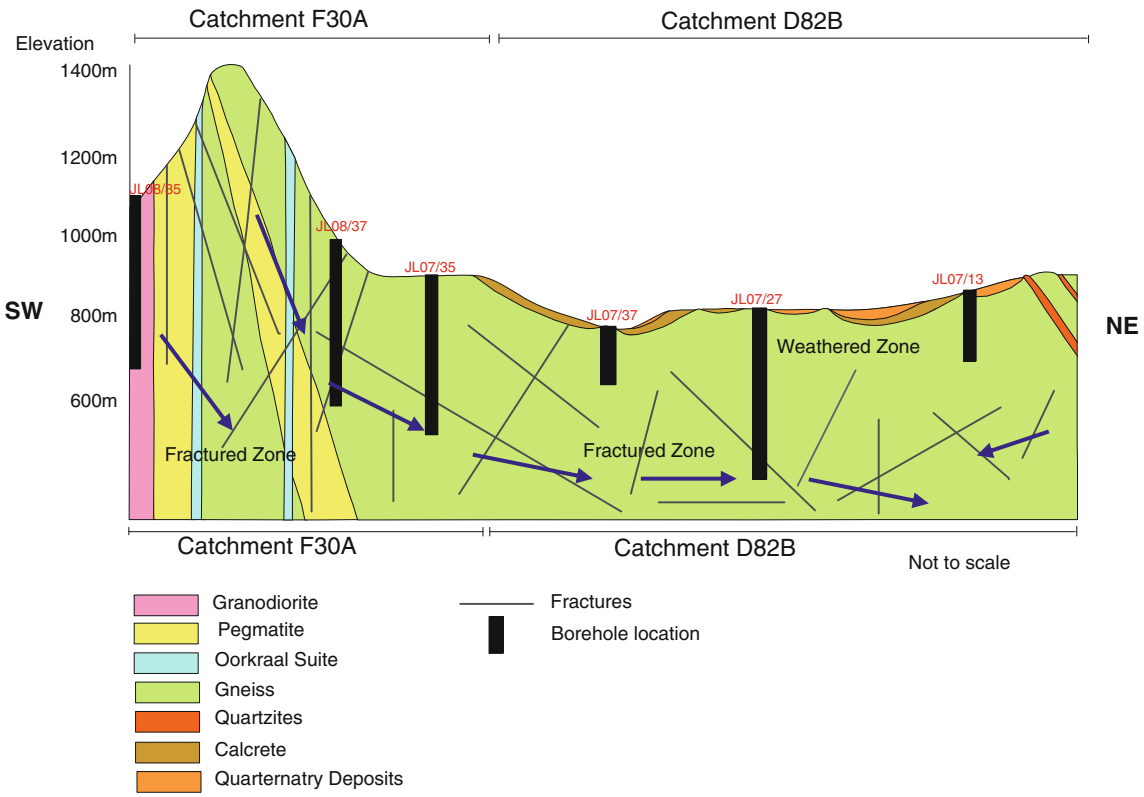

Fig. 3 Conceptual hydrogeological cross-section that depicts groundwater flow between catchments F30A and D82B

The concentration of high total iron in the groundwater (≈940 µg/L in F30A catchment and ≈1110 µg/L in D82B catchment) shows the presence of active oxidation process where water–rock/soil interaction takes place between oxidized ion minerals and organic matter or possibly pyrite oxidation.

High abundance of chromium about 185 µg/L in groundwater could be related to the chromate (Cr_2O_3) mineralization in the crystalline aquifer. Boron concentration is also high, 3018 µg/L, which is related to evaporitic source as witnessed by the widespread salt pans in the area. According to Hem (1992), evaporate areas act as a main source which suggests the direct impact of climatic aridity to its source in agreement with salinity increase. Abundant total chromium (≈470 µg/L) is also attributed to the oxidation process from chromium bearing sediments.

The hydrochemical plot on Fig. 6 reveals the processes that are taking place in the fractured basement aquifers of the area. Groundwater from both catchments plot in fields 3, 5 and 6. The fields are explained by (Lloyd and Heathcote 1985) as follows:

- Field No. 3. HCO_3^- and Na^+ dominant often indicates ion exchanged waters
- Field No. 5. No dominant anions or cations indicates water resulting from dissolution or mixing
- Field No. 6. SO_4^{2-} (or anion indiscriminate) and Na^+ dominant is a water type not frequently found and may be due to mixing influences

The most common water types in the analysed samples are Na–Cl, Na–Ca–Cl, Na–Ca–Cl-HCO_3, Ca–Na-Cl, Na–Ca–Cl-SO_4 and Na–Ca-SO_4 amongst others.

D82B catchment has high EC as a result of mineralization process and with noticeably high nitrate concentration ranging from 4.37 to 448.86 mg/l. There is no clear source of the nitrate source in the area, therefore, the high nitrate concentration is presumed to be natural, since there are no agricultural activities or sewages in the area.

The plot for sulphate versus chloride (Fig. 7) shows a good correlation suggesting that they both results from a common source or processes, e.g. dissolution of evaporites (formed as a result of excessive evaporation in arid climate) particularly in F30A catchment or leaching from host rock. The most likely source of sulphate in the area is from the dissolution of gypsum, oxidation of pyrite and weathering of pegmatites. The plot on Fig. 7 further shows two clusters: the recharging area (catchment F30A) has low Cl and SO_4, while catchment D28B has more enriched concentration. In the catchment D82B, there could be strong pyrite oxidation process than in catchment F30A which contributes to iron and sulphate concentration.

Table 1 Chemical constituents in catchment F30A

Sample ID	JL 07-31	JL 07-33	JL 07-35	JL 07-37	JL 07-39	JL 08-13	JL 08-21	JL 08-25	JL 08-27	JL 08-29	JL 08-31	JL 08-33
pH	7.75	7.77	7.62	8.84	7.27	5.87	6.63	7.11	6.86	6.39	6.38	6.42
Eh (mV)	−31.2	−44.4	−31.8	−98.9	+0.8	+51.3	+44.3	+24.9	+40.2	+70.8	+58.3	+61.9
T (°C)	19.20	19.90	28.00	18.60	23.40	24.50	17.60	20.40	27.10	24.40	26.60	19.20
EC (mS/cm)	1.86	2.28	4.23	2.32	2.02	1.76	1.30	2.26	1.70	1.29	2.64	1.45
TDS (mg/l)	932	1144	2110	1156	1009	601	646	1136	854	643	1316	721
Total Alk (mg/L) $CaCO_3$	310.00	220.00	240.00	170.00	260.00	200.00	227.00	186.00	172.00	73.00	168.00	128.00
Na (mg/l)	305.90	241.60	587.74	353.45	222.76	146.23	145.30	308.30	262.60	177.64	270.79	117.01
Mg (mg/l)	22.34	63.35	82.84	37.81	68.53	34.74	36.87	81.61	47.45	35.82	94.02	58.79
K (mg/l)	15.72	4.30	3.53	19.01	1.75	9.89	9.35	5.10	2.08	1.65	9.67	1.92
Ca (mg/l)	40.28	91.88	89.37	31.19	81.37	70.56	82.92	86.08	54.33	42.81	161.52	102.74
Cl (mg/l)	411.17	600.80	1206.78	543.98	447.21	209.72	298.38	649.28	426.08	364.46	695.36	331.67
NO_3 (mg/l)	7.61	4.37	4.55	8.26	20.20	28.58	9.64	18.78	20.75	6.56	82.62	123.18
PO_4 (mg/l)	2.57	0.00	7.07	0.00	5.00	0.00	0.00	0.00	0.00	0.00	0.00	0.00
SO_4 (mg/l)	112.05	187.06	242.23	191.29	162.32	54.74	69.43	123.66	115.04	97.98	124.25	90.63
U (μg/l)	20.37	6.51	1.00	1.00	1.00	3.41	31.81	1.00	3.43	1.00	5.67	1.00
Zn (μg/l)	487.78	300.00	556.42	300.00	518.65	300.00	442.68	496.92	2023.55	569.94	641.84	1327.91
Fe (μg/l)	881.06	707.59	865.79	598.27	732.56	50.00	50.00	50.00	50.00	50.00	50.00	50.00
Sr (μg/l)	374.62	831.90	681.94	502.12	426.51	500.68	561.84	827.54	352.23	273.05	910.58	680.16
Ag (μg/l)	76.65	24.24	11.04	3.97	1.00	1.00	1.00	1.00	1.00	1.00	1.00	1.00
Cd (μg/l)	1.27	1.00	1.00	1.00	1.00	1.00	1.00	1.00	1.72	1.00	1.00	1.00
Pb (μg/l)	30.00	30.00	30.00	30.00	30.00	30.00	30.00	30.00	30.00	30.00	30.32	30.00
B (μg/l)	869.94	273.58	342.96	832.15	554.41	216.01	334.31	328.23	404.18	200.00	386.86	200.00
Cr (μg/l)	212.13	199.32	205.64	196.55	194.64	2.50	2.50	2.50	2.50	2.50	2.50	2.50
Br (μg/l)	1584.21	2506.63	0.00	1973.13	1985.43	0.00	0.00	0.00	0.00	0.00	0.00	0.00

Sample ID	JL 07-03	JL 07-04	JL 07-43	JL 07-45	JL 08-17	JL 08-23	JL 08-35	JL 08-37	JL-09-17	JL-09-23
pH	7.45	7.28	7.40	7.49	6.80	6.42	6.42	6.01	7.94	8.17
Eh (mV)	14.3−	1.5+	9.8−	22.4−	44.3+	6.4+	71.2+	85.6+	24.1−	34.1−
T (°C)	33.40	24.80	21.70	23.80	25.00	18.80	19.40	25.10	12.50	13.90
EC (mS/cm)	1.51	1.36	1.57	2.05	4.09	6.50	3.68	2.81	0.99	1.62
TDS (mg/l)	752	682	786	1027	2050	3240	162	1385	497	811
Total Alk (mg/L) $CaCO_3$	200.00	114.00	270.00	310.00	202.00	259.00	64.00	134.00	132.00	192.00
Na (mg/l)	218.36	169.88	153.79	241.50	419.63	1081.32	27.92	220.36	123.10	241.80
Mg (mg/l)	35.45	45.87	53.06	55.84	112.56	171.70	6.20	124.53	23.42	31.66
K (mg/l)	4.75	3.57	2.66	9.94	18.02	28.67	1.09	4.98	3.68	1.10
Ca (mg/l)	63.08	72.20	73.26	76.82	349.92	253.05	37.23	189.47	53.61	68.59
Cl (mg/l)	305.97	284.64	312.18	500.50	1278.26	1949.07	62.08	645.07	220.00	411.52
NO_3 (mg/l)	6.36	28.95	25.81	12.91	72.35	29.41	0.00	49.06	26.77	19.21
PO_4 (mg/l)	16.53	10.65	0.00	6.06	0.00	0.00	0.00	0.00	0.00	0.00
SO_4 (mg/l)	98.51	142.23	123.49	148.39	264.23	404.76	43.29	159.03	67.38	112.18
U (μg/l)	12.93	32.91	5.56	8.20	46.75	76.74	3.21	8.74	3.14	8.98
Zn (μg/l)	603.55	1753.95	329.74	300.00	457.57	579.16	300.00	1097.43	1619.41	1487.63
Fe (μg/l)	383.38	387.16	939.99	779.94	50.00	50.00	50.00	50.00	50.00	316.64
Sr (μg/l)	330.42	388.20	350.80	457.39	2405.05	2691.46	68.84	906.78	340.31	331.77
Ag (μg/l)	1.00	1.00	1.00	1.00	1.00	1.00	1.00	1.00	1.00	1.00
Cd (μg/l)	1.00	2.60	1.00	1.00	1.00	1.51	1.00	1.00	2.61	2.11
Pb (μg/l)	110.12	294.83	30.00	30.00	30.00	30.00	30.00	30.00	30.00	30.00
Cr (μg/l)	2.50	2.50	222.52	214.62	2.50	2.50	2.50	2.50	2.50	4.74
B (μg/l)	738.44	544.84	418.81	490.14	707.10	1635.10	200.00	200.00	254.99	366.82
Br (μg/l)	0.00	0.00	0.00	0.00	0.00	0.00	0.00	0.00	0.00	0.00

Table 2 Chemical constituents in catchment D82B

Sample ID	JL 07-01	JL 07-02	JL 07-09	JL 07-11	JL 07-13	JL 07-15	JL 07-17	JL 07-19	JL 07-21	JL 07-23	JL 07-25	JL 07-27
pH	7.29	7.91	4.90	6.72	7.11	7.64	7.78	7.20	7.22	7.17	7.37	7.92
Eh (mV)	−2.1	−40.3	+117.4	+2.3	+1.0	+38.7	−34.5	−1.7	−2.4	−11.7	−11.1	−52.9
T (°C)	22.30	23.60	23.20	20.90	21.50	17.20	19.10	22.70	17.00	31.70	18.40	16.80
EC (mS/cm)	3.36	3.73	3.60	5.82	2.75	12.13	1.49	4.58	3.72	6.41	10.29	4.62
TDS (mg/l)	1678	1879	1814	2920	1375	6070	746	2290	1863	3180	5150	2320
Total Alk (mg/L) $CaCO_3$	190.00	200.00	250.00	220.00	280.00	250.00	190.00	220.00	270.00	220.00	230.00	260.00
Na (mg/l)	350.34	605.91	303.61	652.63	318.09	1802.00	178.20	568.26	383.29	960.26	1463.81	535.42
Mg (mg/l)	55.49	52.18	78.02	109.15	51.25	217.34	34.13	84.87	69.65	101.02	147.74	111.37
K (mg/l)	19.92	30.59	25.04	39.73	17.46	55.14	21.01	22.71	26.26	44.30	56.99	26.78
Ca (mg/l)	162.07	154.91	267.22	398.53	173.17	579.32	71.38	300.19	277.65	268.33	602.81	227.63
Cl (mg/l)	820.78	875.27	800.15	1553.45	556.69	2591.91	308.61	1074.98	896.11	1785.41	2994.41	1291.23
NO_3 (mg/l)	70.86	114.66	167.66	128.17	141.06	238.23	83.48	256.87	225.44	161.91	448.86	42.90
PO_4 (mg/l)	267.95	14.19	32.42	0.00	8.46	0.00	4.22	11.16	13.49	56.47	34.69	10.15
SO_4 (mg/l)	210.71	309.99	433.23	602.87	290.32	666.98	103.41	468.78	306.33	792.64	879.11	366.18
U (μg/l)	45.86	66.46	145.99	24.26	49.66	88.29	19.72	104.41	27.18	69.24	60.81	11.98
Zn (μg/l)	395.83	584.13	300.00	300.00	667.80	300.00	300.00	300.00	300.00	568.90	300.00	300.00
Fe (μg/l)	434.43	1011.18	693.21	556.32	585.47	692.77	708.99	789.91	894.39	727.83	835.11	526.98
Sr (μg/l)	1597.98	1932.25	2266.16	5708.40	1597.74	7805.18	645.17	3063.69	1950.89	3601.74	8307.77	2253.86
Ag (μg/l)	1.60	1.06	27.68	15.46	4.65	7.69	1.00	1.00	1.00	1.00	1.00	1.00
Cd (μg/l)	1.00	1.18	1.00	1.00	1.00	1.00	1.00	1.00	1.00	1.00	1.00	1.00
Pb (μg/l)	88.68	42.32	30.00	30.00	30.00	30.00	30.00	30.00	30.00	30.00	30.00	30.00
Cr (μg/l)	2.50	2.50	174.00	207.17	207.58	188.13	208.16	211.61	224.49	213.79	218.32	198.13
B (μg/l)	1025.82	2208.65	752.92	1479.74	1072.46	2091.40	608.48	1859.79	1053.95	2150.35	3018.95	1326.42
Br (μg/l)	0.00	3257.19	5340.78	9068.03	3241.15	0.00	1303.98	4701.27	0.00	0.00	0.00	5284.58

Sample ID	JL 07-29	JL 07-41	JL 07-47	JL 07-49	JL 07-51	JL 08-01	JL 08-03	JL 08-05	JL 08-07
pH	7.42	7.27	7.42	7.10	7.22	6.39	5.75	6.27	6.22
Eh (mV)	−16.4	−22.8	−14.1	−3.0	−2.9	+46.3	+87.2	+68	+75.5
T (°C)	23.50	33.20	19.80	20.20	20.70	19.10	21.20	26.60	22.80
EC (mS/cm)	3.33	1.17	5.64	12.88	10.62	1.71	6.57	1.38	2.06
TDS (mg/l)	1667	585	2820	6430	5310	856	3270	689	1032
Total Alk (mg/L) $CaCO_3$	130.00	240.00	230.00	290.00	270.00	111.00	167.00	223.00	220.00
Na (mg/l)	422.30	111.99	609.69	1960.35	1523.02	217.94	901.37	155.41	203.86
Mg (mg/l)	72.30	31.64	139.05	269.36	156.41	41.30	127.27	23.38	49.71
K (mg/l)	18.47	4.08	30.40	75.62	47.51	10.93	38.66	14.42	13.35
Ca (mg/l)	169.72	57.00	332.32	451.13	536.18	89.48	450.99	110.39	167.87
Cl (mg/l)	707.56	240.23	1638.20	4070.03	3149.20	424.22	2057.66	288.96	468.47
NO_3 (mg/l)	139.60	32.04	60.79	206.98	232.85	50.58	56.07	70.34	97.18
PO_4 (mg/l)	5.81	0.00	7.37	0.00	0.00	0.00	0.00	0.00	0.00
SO_4 (mg/l)	372.30	83.63	296.44	993.65	1005.32	152.12	319.98	90.25	174.18
U (μg/l)	11.64	2.84	11.14	34.47	23.86	10.36	32.14	22.09	41.43
Zn (μg/l)	1178.11	300.00	387.84	1609.70	454.42	1014.04	300.00	982.92	314.97
Fe (μg/l)	1113.74	846.87	876.61	817.69	962.24	50.00	50.00	50.00	50.00
Sr (μg/l)	1409.97	293.09	2716.36	8051.17	6899.02	950.37	4131.47	647.37	1170.44
Ag (μg/l)	1.00	1.00	1.00	1.00	1.00	1.00	1.00	1.00	1.00
Cd (μg/l)	1.00	1.00	1.00	1.00	1.00	1.04	1.00	1.00	1.00
Pb (μg/l)	30.00	30.00	30.00	30.00	40.00	50.21	30.00	30.00	30.00
Cr (μg/l)	228.56	214.02	215.80	198.49	470.72	2.50	2.50	2.50	2.50
B (μg/l)	1832.13	250.37	1233.74	4494.86	3102.13	307.19	1319.09	422.97	518.81
Br (μg/l)	0.00	0.00	5280.19	15270.63	0.00	0.00	0.00	0.00	0.00

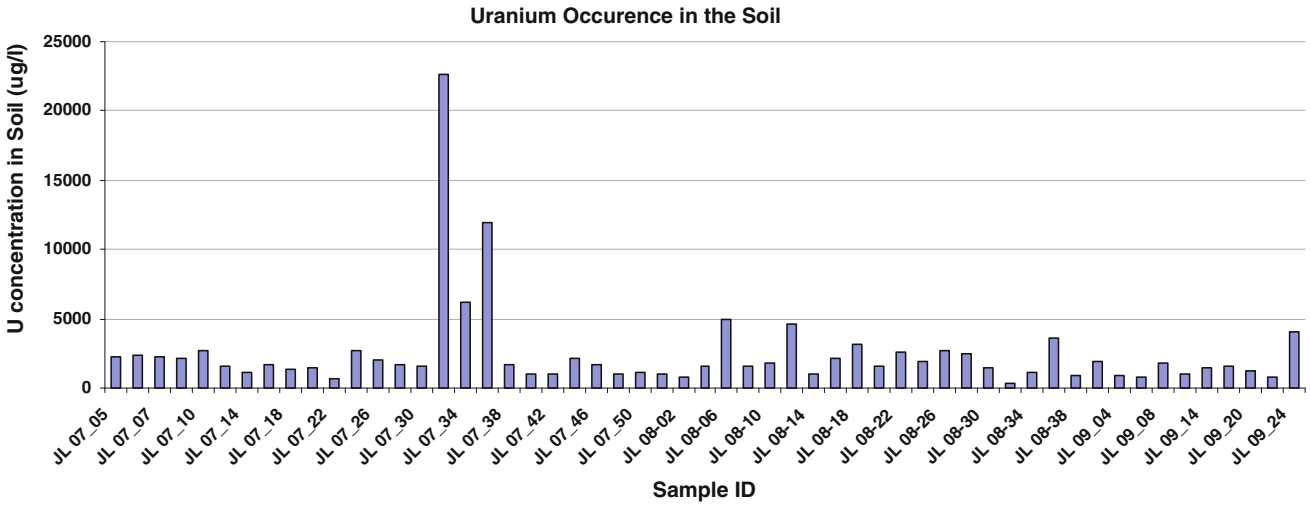

Fig. 4 Uranium concentration in soil samples from F30A and D82B catchments

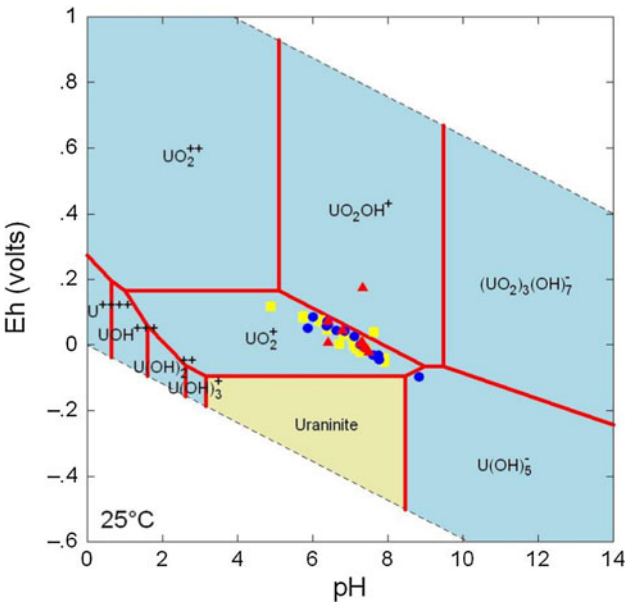

Fig. 5 Uranium stability field

Bromide and chloride are conservative elements and, therefore, can be used to define processes such as mixing, evaporation among others. Bromide concentration in groundwater is generally low, but high concentrations of this element sometimes occur in groundwater by pollution, interaction with seawater or reaction with evaporite deposits (Mokrik et al. 2005). Br^- versus Cl^- diagrams were plotted to establish the source of salinity in the groundwater samples (Fig. 8). The diagram reveals that source of salinity is controlled by evaporite dissolution and mixing in the D82B catchment, while atmospheric deposition or sea aerosols spray seems responsible in F30A catchment.

The Br/Cl ratio for most of the samples exceed the marine ratio of 0.0035 (Fig. 9) and this means that the groundwater could originate from marine formations (Edmunds et al. 2006). The occurrence of high chloride concentrations in some groundwater samples from F30A catchment coincides with an area close to D82B catchment. The plots on Fig. 8 and 9 show that the salinity in the area is derived from sea water mixing, halite dissolution and atmospheric deposition/sea aerosol spray. Under excessive evaporative regimes, as experience in arid environments, some of the groundwater is heading towards hypersaline waters especially that of D82B catchment. The F30A catchment seems to have its Cl and Br ions derived from atmospheric deposition/sea aerosol spray, with some of the samples showing salinity from seawater intrusion/halite dissolution.

Environmental isotopes

Twenty-four groundwater samples were analysed for stable isotopes and tritium. Groundwater from the two catchments (F30A and D82B) shows that tritium concentration is substantially very low with the majority that falls below 0.6 T.U. (Table 3), indicating old water recharged prior to the era of thermonuclear bomb testing and lack of modern water recharge.

The stable isotope plot (Fig. 10) indicates that groundwater samples from catchment D82B plots away from the GMWL showing isotope enrichment due to evaporation prior to recharge (plotted on evaporation line) which has been supported by high EC due to mineralization and high salinity occurrence. F30A samples show infiltration from direct precipitation which could occur on high altitude (adjacent) areas as there is erratic local rainfall in the area.

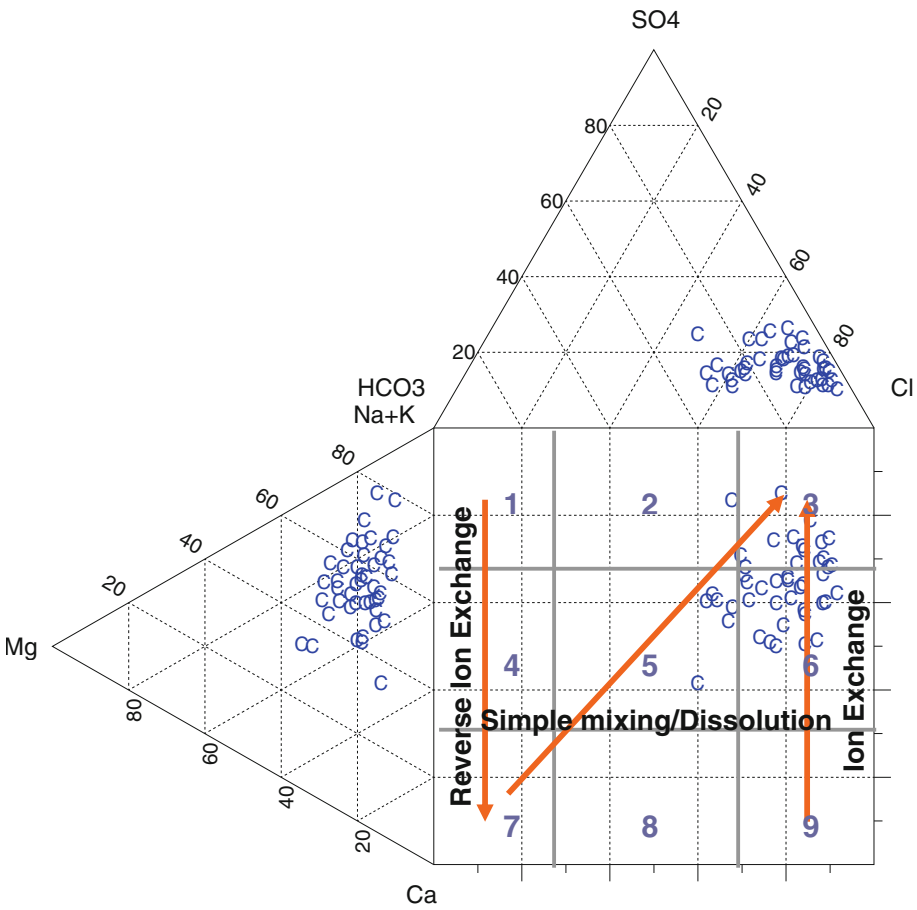

Fig. 6 Durov diagram for the groundwater samples in the area showing geochemical evolution trend

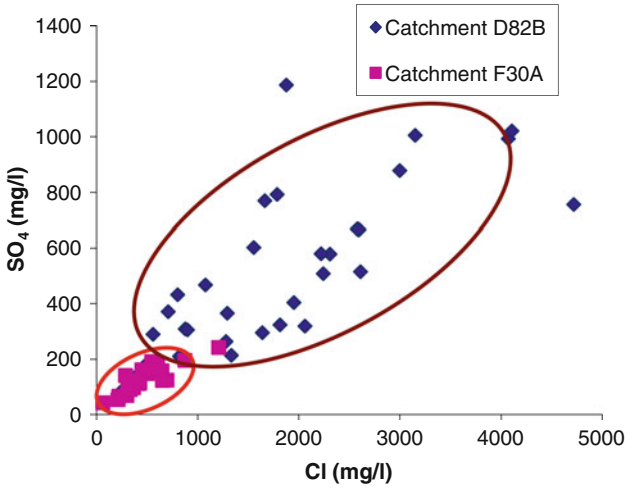

Fig. 7 Sulphate versus chloride diagram

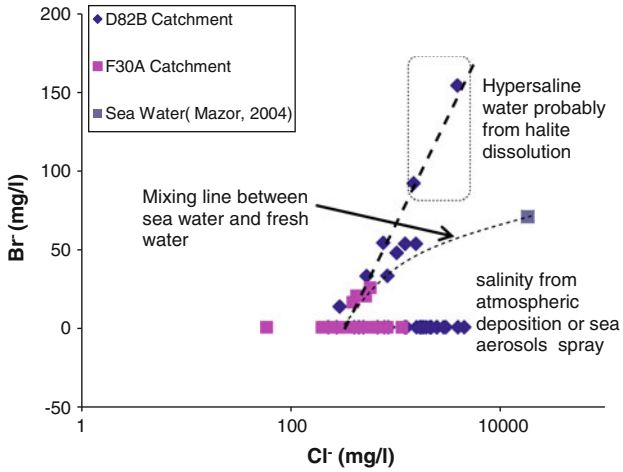

Fig. 8 Br^- versus Cl^- plot

The widely distributed tritium values (0–2 TU) in catchment F30A and D82B implies comparatively higher level of recharge than the D82B catchment (Fig. 11) or the possibility of inter-basin water transfer through tectonic structures. The older groundwaters with tritium value of 0.0 TU in the area could result from upwelling of old groundwater from the granites and/or metamorphic bodies. Moreover, the variation in tritium values may be attributed to flow direction and velocities within faults and fractures in the area. Fracturing and faulting may lead to mixing of waters from different aquifer units. Mixing between highly saline or brine with modern meteoric water in the area is demonstrated by the decrease in salinity in most boreholes (Clark and Fritz 1997). Fig. 11 shows three distinct groundwaters in the area.

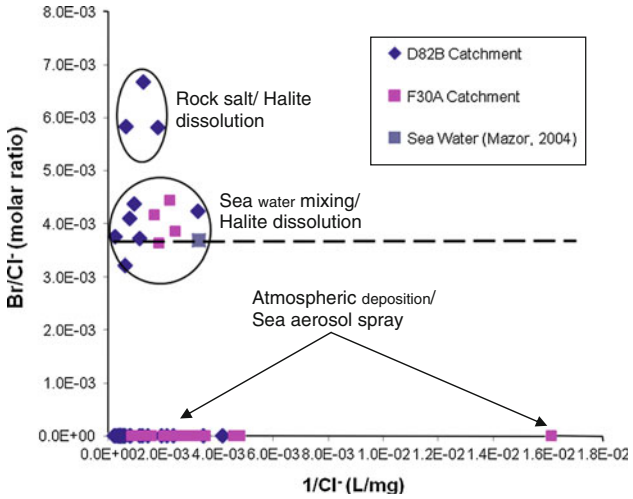

Fig. 9 Br^-/Cl^- versus $1/Cl^-$

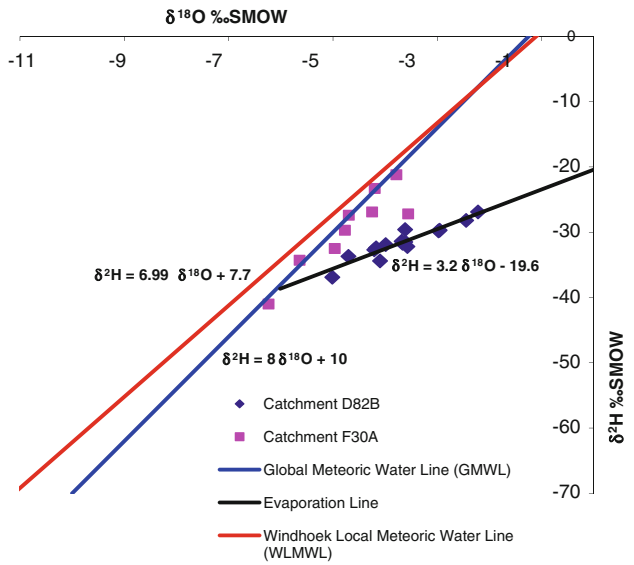

Fig. 10 Stable isotope plot relative to global meteoric water line (Craig 1961) and Windhoek local meteoric water line

Table 3 Environmental Isotope values for the groundwater of the area

Sample ID	δD (‰)	δ18O (‰)	3H(T.U.)
JL 07/13 Neelsvlei	-36.9	-5.01	1.2±0.3
JL 08/01 Oubip Farm	-33.7	-4.70	0.0±0.2
JL 08/03 Bosluis	-34.4	-4.10	0.3±0.2
JL 08/05 Naroegas	-32.4	-4.17	0.9±0.2
JL 08/07 Heuningvlei	-31.5	-3.62	2.0±0.3
JL08/09 Frummel Bakkies	-28.2	-2.45	1.0±0.3
JL 08/13 Wolfkraal	-27.2	-3.56	0.0±0.2
JL 08/17 Driehoek	-31.9	-3.99	0.0±0.2
JL 08/21 Kamiebees	-29.7	-4.77	0.2±0.2
JL 08/23 Bokseputs	-29.6	-3.62	0.5±0.2
JL 08/25 Kaams	-32.5	-4.97	0.2±0.2
JL 08/29 Riet	-34.3	-5.64	0.6±0.2
JL 08/33 Pedro's Kloof	-21.1	-3.79	1.7±0.3
JL08/37 Couragie Fontein	-26.9	-4.25	1.3±0.3
JL 09/01 Spioenkop	-26.9	-2.22	0.3±0.2
JL 09/03 Rooiduin 1	-31.7	-3.67	0.6±0.2
JL 09/05 Rooiduin 2	-32.2	-3.57	0.0±0.2
JL 09/07 Diepvlei	-29.7	-2.96	0.6±0.2
JL 09/09 Uitkyk	-29.8	-2.98	0.0±0.2
JL 09/11 Katvlei 2	-32.7	-4.21	0.0±0.2
JL 09/15 Mannsepan	-31.4	-3.68	0.2±0.2
JL 09/17 Tweefontein	-41.0	-6.24	0.5±0.2
JL 09/19 Nuwedam	-23.3	-4.20	1.7±0.3
JL 09/23 Stofkraal	-27.4	-4.70	1.7±0.3

1. Group 1: deep circulating water characterised by high Cl concentration <1000 mg/l and low tritium values of <0.8 TU. The groundwater with low tritium units and higher chloride concentration is from the low lying or flat areas of the study area indicating groundwater which underwent sever evaporation before and/or during recharge. Low tritium values could indicate low permeability of rocks, water that has travelled long distance from highland recharge areas, or in general old water that is in circulation for over six decades and occur in D82B catchment.

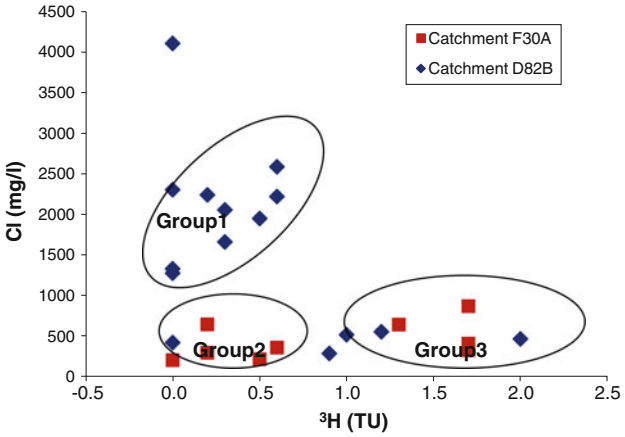

Fig. 11 Groundwater clusters in the area

2. Group 2: deep circulating groundwater, characterised by Cl values <1000 mg/l and a range of tritium values of <0.8 TU. These samples are mostly from F30A catchment.
3. Group 3: shallow circulating groundwater, characterised by low chloride and low tritium content (up to 2 TU). This group is presumed to be derived from water that recharges during summer season when rainfall is high.

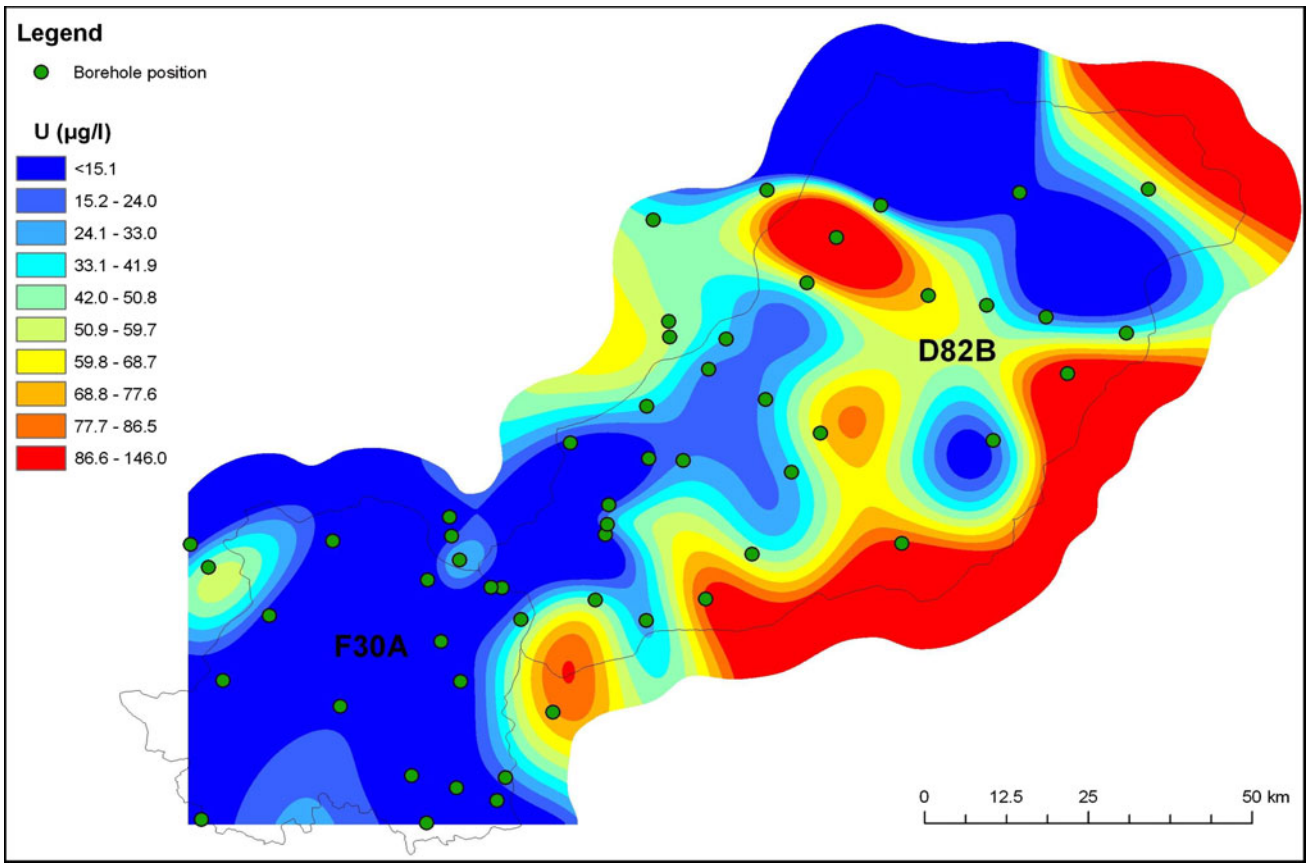

Fig. 12 Spatial distribution of the uranium in groundwater

Spatial distribution of uranium is portrayed in Fig. 12 where concentration increase is noticeable in D82B catchment. The highest concentration of uranium was detected in borehole JL07/09 (146 µg/l), JL07/19 (104 µg/l), JL08/11 (88 µg/l) and JL 08/23 (77 µg/l), respectively, which lie in the discharging area of catchment D82B (Fig. 12). A spatial distribution further reveals that the groundwater in catchment F30A has low uranium concentrations (mostly, <15.1 µg/l), while high uranium concentration is evident in the catchment D82B of up to 146 µg/l which could be attributed to long residence time.

Radiological aspect

A gross alpha analysis yields an estimate of the total alpha emissions from all decaying radionuclides in a sample, but does not speciate radiological constituents (Ainslie 2003). The analytical result in Table 4 revealed the presence of radiometric anomalies in the groundwater of the area. Of course, groundwater is the main pathway for the transport of radioactivity to the consumers from groundwater. Some studies (Andreoli et al. 2004, 2006) show that the K, U and Th values for rocks of the metamorphic complex are sufficient to explain the elevated airborne radiometric anomalies in Namaqualand. It was also noted that U and Th are largely hosted by igneous and high-grade metamorphic minerals, mainly zircon and monazite (Andreoli et al. 2006). The radiometric anomalies in the area are related to the emplacement history of the igneous host rocks or to metamorphic processes in the granulite-facies (Andreoli et al. 2004).

Gross alpha and beta emitters were detected in the water samples and are also likely attributed to naturally occurring uranium isotopes present in the water. The results show that in the groundwater of the two catchments, the gross alpha activity in Liquid residuals falls between −0.082 and 18.2 Bq/L. According to the South African Water quality guideline [DWAF (Department of Water Affairs and Forestry) 1996], the limiting range for alpha activity for domestic use is between 0 and 0.5 Bq/L. In this regard, 41 % of the reported data in Table 4 fall above the limit.

Conclusion

Groundwater chemistry in the two catchments (F30A and D82B) is variable with clear evolutionary trend where groundwater flows from catchment F30A to catchment

Table 4 Gross alpha and beta activity of the liquid residuals (Bq/l)

Sample ID	Gross alpha-activity			Gross beta-activity		
	Value	Unc.	MDA	Value	Unc.	MDA
JL 07/09	2.25	±0.39	1.2	1.69	±0.12	0.21
JL 07/11	0.573	±0.561	1.9	1.52	±0.12	0.22
JL 07/13	1.67	±0.33	1	1.14	±0.1	0.21
JL 07/15	2.2	±0.61	1.9	2.14	±0.15	0.22
JL 07/17	0.721	±0.266	0.86	0.893	±0.086	0.21
JL 07/19	4.84	±0.52	1.3	1.51	±0.11	0.22
JL 07/23	2.56	±0.55	1.7	1.7	±0.13	0.22
JL 07/27	0.334	±0.446	1.5	1.1	±0.1	0.22
JL 07/21	0.135	±0.172	0.57	0.0874	±0.063	0.2
JL 07/25	1.13	±0.45	1.5	2.15	±0.14	0.22
JL 07/29	0.269	±0.261	0.86	0.512	±0.076	0.21
JL 07/31	0.868	±0.236	0.75	0.731	±0.081	0.21
JL 07/33	0.259	±0.227	0.75	0.617	±0.077	0.21
JL 07/35	0.0753	±0.3544	1.2	1.49	±0.11	0.21
JL 07/37	−0.0026	±0.2553	0.86	0.975	±0.087	0.21
JL 07/39	−0.0431	±0.2481	0.84	0.263	±0.069	0.21
JL 07/43	0.136	±0.255	0.85	0.285	±0.07	0.21
JL 07/47	0.303	±0.454	1.5	0.903	±0.093	0.22
JL 07/49	0.327	±0.439	1.5	1.68	±0.12	0.22
JL 07/51	0.579	±0.449	1.5	2.19	±0.14	0.22
JL 07/41	0.0634	±0.2053	0.69	0.229	±0.067	0.2
JL 07/45	0.281	±0.315	1	0.547	±0.078	0.21
JL 08/01	0.39	0.38	1.3	0.6	0.34	1.1
JL 08/03	−0.28	1.02	3.4	2.01	0.39	1.2
JL08/05	1.2	0.4	1.3	17.5	0.7	1.1
JL 08/07	1.2	0.5	1.7	3.01	0.37	1.1
JL 08/09	1.2	0.6	2	1.1	0.4	1.2
JL 08/11	2.4	0.8	2.5	37.4	1.6	1.2
JL 08/13	−0.082	0.32	1.1	0.65	0.34	1.1
JL 08/15	1	0.6	2.1	2.39	0.37	1.2
JL 08/17	1.4	0.8	2.6	1.22	0.37	1.2
JL 08/19	0.3	1.31	4.4	7.32	0.63	1.6
JL 08/21	1.25	0.38	1.2	0.63	0.34	1.1
JL 08/23	12.7	0.9	2.1	283	10	1.2
JL 08/25	18.2	1	1.7	590	20	1.1
JL 08/27	−0.22	0.35	1.2	0.15	0.34	1.1
JL 08/29	−0.22	0.36	1.2	0.37	0.34	1.1
JL 08/31	−0.36	0.53	1.8	0.33	0.35	1.1
JL 08/33	0	0.37	1.3	0.52	0.34	1.1
JL 08/35	0.12	0.23	0.77	18.6	0.7	1.1
JL 08/37	−0.38	0.57	1.9	0.83	0.35	1.2

D82B. The processes that might control the ion enrichment are dissolution, redox, evaporation and the long residence time, which promote water–rock interaction. The area, generally, has poor water quality due to geogenic sources of chemical constituents especially toxic trace metals such as uranium. The range of groundwater composition in the aquifer suggests varying influences of evaporite dissolution, carbonate or silicate weathering. Sulphate and chloride, dominated groundwater composition, are attributable to pyrite oxidation, gypsum and halite dissolution. Br^-/Cl^- ratio show that the salinity in the area results from sea water mixing, halite dissolution and atmospheric deposition/sea aerosol spray. The stable isotope results instead indicate that the samples have undergone fractionation due to evaporation before infiltration especially in catchment D82B. The results further revealed that there is a mixing process of groundwater in the aquifer (deep circulating and shallow groundwater). In comparison to the South African water quality standard, the results obtained for Gross alpha activity show that 41 % of the reported data in the area fall above the limit.

Acknowledgments The authors would like to thank the Council for Geosciences (CGS) of South Africa for data collection and analyses. The constant support of National Research Foundation (NRF) is high appreciated for strengthening the Hydrogeology research component at Wits University, Johannesburg.

References

Agenbacht ALD (2007) The geology of the Pofadder area. Explanation Sheet 2918, 1:250 000

Ainslie LC (2003) Influence of waste disposal operations on the radiological environment at Vaalputs. South African Nuclear Energy Cooperation (NECSA), Document number: GEA-1638

Albat HM (1984) The Proterozoic granulite facies terrane around Kliprand, Namaqualand Metamorphic Complex. Ph.D. Thesis, Dept. of Geology, University of Cape Town, South Africa. In: Chamber of Mines Precambrian Research Unit. Bulletin 33

Andreoli MAG, Smith CB, Watkeys M, Moore JM, Ashwal LD, Hart RJ (2004) The geology of the Steenkampskraal monazite deposit, South Africa: implications for REE-Th-Cu mineralization in charnockite-granulite terranes. Econ Geol 89(5):994–1016

Andreoli MAG, Hart RJ, Ashwal LD, Coetzee H (2006) Correlation between U, Th content and metamorphic grade in the western Namaqualand belt, South Africa, with implications for radioactive heating of the crust. J Petrol 47(6):1095–1118

Bonotto DM, Bueno TO (2008) The natural radioactivity in Guarani aquifer groundwater, Brazil. Appl Radiat Isotopes 66:1507–1522

Bonotto DM, Bueno TO, Tessari BW, Silva A (2009) The natural radioactivity in water by gross alpha and beta measurements. Radiat Meas 44:92–101

Clark I, Fritz P (1997) Environmental isotopes in hydrogeology. Lewis Publishers, New York, p 328

Cole DI (1998) Uranium in "The Mineral Resources of South Africa". In: Wilson MGC, Anhaeusser CR (eds) Handbook, Council for Geoscience. 16:642–658

Craig H (1961) Isotopic variations in meteoric waters. Science 133:1702–1703

DWAF (2002) Lower Orange Water Management Area: Water resources situation assessment. Compiled by V3 Consulting Engineers, assisted by Water Resource Planning and Conservation. South Africa, Report number 14000/00/0101

DWAF (Department of Water Affairs and Forestry) (1996) South African Water quality guideline. Second edition. V1. Domestic use. P214

Edmunds WM, Ma J, Aeschbach-Hertig W, Kipfer R, Darbyshire DPF (2006) Groundwater recharge history and hydrogeochemical evolution in the Minqin basin, North West China. Applied Geochemistry 21: 2148–2170

Frick C (1986) The behaviour of uranium, thorium and tin during leaching from a coarse grained porphyritic granite in arid environment. Journal of Geochemical Exploration 25(3): 261–282

Hem J (1992) Study and interpretation of the chemical characteristics of natural water. USGS water supply paper 2254

Kim Y, Park H, Kim J, Park S, Cho B, Sung I, Shin D (2004) Health risk assessment for uranium in Korean groundwater. J Environ Radioact 77:77–85

Kleinschmidt R, Black J, Akber R (2011) Mapping radioactivity in groundwater to identify elevated exposure in remote and rural communities. J Environ Radioact 102:235–243

Langmuir D (1980) Uranium solution-mineral equilibria at low temperatures with applications to sedimentary ore deposits. Geochim Cosmochim Acta 42:547–569

Lloyd JW, Heathcote JA (1985) Natural inorganic hydrochemistry in relation to groundwater. An introduction. Claredon Press, Oxford

Mokrik R, Savitskaja L, Savitski L (2005) Aqueous geochemistry of the Cambian-Vendian aquifer system in the Tallinn intake, northern Estonia. Geologija, No. 51, pp 50–56. Available on line

Murphy WM, Shock EL (1999) Environmental aqueous geochemistry of actinides. In: Burns PC, Finch R (eds) Uranium: mineralogy, geochemistry and the environment. Mineralogical Society of America, Chantilly, pp 221–254

Nriagu J, Nam D-H, Ayanwola TA, Dinh H, Erdenechimeg E, Ochir C, Bolormaa T-A (2012) High levels of uranium in groundwater of Ulaanbaatar, Mongolia. Sci Total Environ 414:722–726

Örgün Y, Altınsoy N, Gültekina AH, Karahanc G, Çelebic N (2005) Natural radioactivity levels in granitic plutons and groundwaters in Southeast part of Eskisehir, Turkey. Appl Radiat Isotopes 63:267–275

Osman AAA, Salih I, Shaddad IA, El Din S, Siddeeg MB, Eltayeb H, Idriss H, Hamza W, Yousif EH (2008) Investigation of natural radioactivity levels in water around Kadugli, Sudan. Appl Radiat Isotopes 66:1650–1653

Plastino W, Povinec PP, De Luca G, Doglioni C, Nisi S, Ioannucci L, Balata M, Laubenstein M, Bella F, Coccia E (2009) Uranium groundwater anomalies and L'Aquila earthquake, 6th April 2009 (Italy). J Environ Radioact 101:45–50

Raith JG, Cornell DH, Frimmel HE, De Beer CH (2003) New insight into the geology of the Namaqua Tectonic Province, South Africa, from ion probe dating of ditrital and metamorphic zircon. J Geol 3(3):347–366

Tankard AJ, Jackson MP, Eriksson KA, Hobday DK, Hunter DR, Minter WEL (1982) Crustal evolution of South Africa: 3.8 billion years of earth history. Springer, New York

Titus R, Xu Y, Adams S, Beekman H (2009) A tectonic and geomorphic framework for the development of basement aquifers of Namaqualand–a review. In: Titus R, Beekman R, Adams S, Strachan L (eds) "The Basement Aquifers of Southern Africa". WRC Report TT 428/09. ISBN 978-1-77005-898-9

Toens PD, Stadler W, Wullschleger NJ (1998) The association of groundwater chemistry and geology with atypical lymphocytes (as a biological indicator) in the Pofadder Area, North Western Cape, South Africa. WRC Report 839/1/98, Water Research Commission, Pretoria

Visser DJL (ed) (1989) Explanation of the 1:1.000.000 geological map, fourth edition, 1984. Department of Mineral and Energy Affairs, Government Printer. ISBN 0-621-12516-4

WHO (World Health Organization) (2006) Guidelines for drinking-water quality, vol 1, 3rd edn. Recommendations, Geneva. ISBN 92 4 154696 4